Safe Decision-Making in Interactive Environments

Yorie Nakahira (PI) (https://orcid.org/0000-0003-3324-4602)
Hiraku Hoshino (https://orcid.org/0000-0003-2487-8320)

FINAL REPORT
July 31, 2024

Contents

Chapter 1

Introduction

1.1 Background

Risk quantification and reachability analysis are crucial for safety-critical autonomous control systems. For example, these techniques are widely used in stochastic safe control [1, 2], safe exploration [3, 4], and safe reinforcement learning [5,6,7,8]. However, it is challenging to accurately quantify long-term risks and find maximally safe control policies for complex nonlinear systems. There are stringent trade-offs between accuracy, time horizon, sample complexity, and computation. Such tradeoffs are particularly stringent when the risk is associated with rare events and the dimensions of the systems are high [9]. In addition, unsafe events, risky states, and long-term trajectories can be prohibitively costly to sample from physical systems. Motivated by these challenges, this paper proposes an efficient Physics-Informed Reinforcement Learning (PIRL) that can estimate long-term maximal safety probabilities with *short-term* data that do *not* contain many unsafe events.

1.2 Related work

Many learning-based techniques were developed to quantify various forms of risk. For deterministic systems (worst-case framework), RL techniques were adapted for reachability analysis [10]. For stochastic systems, policy gradient approaches were used to minimize CVaR and coherent risk measures [11]. Deep Q-learning was used to learn the probabilities of constraint violations of time horizon one (at each time), which are then used to constrain learning

and exploration [5, 8]. Estimation of long-term probabilities under maximally safe actions is an optimization problem with multiplicative costs over time whose optimality conditions were characterized [12]. However, solving such optimization problems is not trivial, particularly for high-dimensional systems. Although techniques such as taking logarithms are often used to convert multiplicative costs into summations in practice, such techniques cannot be used directly in this setting (Remark 1 for details). Here, we show that long-term safety probabilities (in the form of multiplicative costs of expected index functions) are transferable to additive costs, for which many RL methods can be used.

Although RL has the potential to offer scalable risk quantification techniques, one may not know how accurate the converged solutions and generalization to states or time horizons whose samples are unavailable. This is problematic if the quantified risk is to be used in safety-critical systems, because the safety of subsequent decision-making techniques depends on accurate risk quantification. To tackle these challenges, we propose to leverage Physics-Informed Neural Networks (PINN) [13]. PINN has a demonstrated potential in generalization due to the use of physics constraints [14, 15]. PINN-based approach has been used to quantify safety probabilities of a given controller with provable generalization [16]. Here, we derive a PDE characterizing the safety probability and integrate it into a PIRL framework.

Due to the integration of RL and PINN, the proposed framework has the following advantages.

- Expansion of feasible regions: By exploring a maximally safe controller, the set of state spaces with tolerable risks is expanded. When the maximal safety probability is used to constrain action and exploration, the system is expected to be less conservative (see Fig. 4.1).

- Learning from sparse rewards in space and time: The proposed method can learn from binary rewards that are also sparse in time and achieve objectives similar to reward shaping (see Fig. 4.3). This is achieved by leveraging physics constraints to extract and propagate information from neighbors and boundaries.

- Generalization to longer-horizon and unsampled risky states: The proposed method can estimate long-term safety probability using short-term samples and achieve comparable learning effect using reduced number of unsafe events (see Fig. 4.4). This feature is beneficial when

samples from long-term trajectories are unavailable or when risky states are costly to sample.

The proposed method is built on Deep Q-Network (DQN) algorithm [17], but the framework is generalizable to other deep RL techniques. While several PIRL frameworks have been proposed (see [18] for a review), to the best of our knowledge, this work is the first to combine an RL problem with PINN for the purpose of estimating maximal safety probabilities and the corresponding policies.

1.3 Notation

Let $\mathbb{R}$ and $\mathbb{R}_+$ be the set of real numbers and the set of nonnegative real numbers, respectively. Let $\mathbf{Z}$ and $\mathbf{Z}_+$ be the set of integers and the set of nonnegative integers. For a set A, A^{c} stands for the complement of A, and ∂A for the boundary of A. Let $\lfloor x \rfloor \in \mathbf{Z}$ be the greatest integer less than or equal to $x \in \mathbb{R}$. Let $\mathbb{1}[\mathcal{E}]$ be an indicator function, which takes 1 when the condition $\mathcal{E}$ holds and otherwise 0. Let $\mathbb{P}[\mathcal{E}|X_0 = x]$ represents the probability that the condition $\mathcal{E}$ holds involving a stochastic process $X = \{X_t\}_{t\in\mathbb{R}_+}$ conditioned on $X_0 = x$. Given random variables X and Y, let $\mathbb{E}[X]$ be the expectation of X, and $\mathbb{E}[X|Y = y]$ be the conditional expectation of X given $Y = y$. We use upper-case letters (*e.g.*, Y) to denote random variables and lower-case letters (*e.g.*, y) to denote their specific realizations. For a scalar function ϕ, $\partial_x \phi$ stands for the gradient of ϕ with respect to x, and $\partial_x^2 \phi$ for the Hessian matrix of ϕ. Let $\mathrm{tr}(M)$ be the trace of the matrix M.

Chapter 2

Problem Statement

We consider a control system with stochastic noise of w-dimensional Brownian motion $\{W_t\}_{t\in\mathbb{R}_+}$ starting from $W_0 = 0$. The system state $X_t \in \mathbb{X} \subset \mathbb{R}^n$ evolves according to the following stochastic differential equation (SDE):

$$\mathrm{d}X_t = f(X_t, U_t)\mathrm{d}t + \sigma(X_t, U_t)\mathrm{d}W_t, \tag{2.1}$$

where $U_t \in \mathbb{U} \subset \mathbb{R}^m$ is the control input. Throughout this paper, we assume sufficient regularity in the coefficients of the system (2.1). That is, the functions f and σ are chosen in a way such that the SDE (2.1) admits a unique strong solution (see, e.g., Section IV.2 of [19]). The size of $\sigma(X_t)$ is determined from the uncertainties in the disturbance, unmodeled dynamics, and prediction errors of the environmental variables.

For numerical approximations of the solutions of the SDE and optimal control problems, we consider a discretization with respect to time with a constant step size Δt under piecewise constant control processes. For $0 = t_0 < t_1 < \cdots < t_k < \ldots$, where $t_k := k\Delta t$, $k \in \mathbf{Z}_+$, by defining the discrete-time state $X_k := X_{t_k}$ with an abuse of notation, the discretized system can be given as

$$X_{k+1} = F^u(X_k, \Delta W_k), \tag{2.2}$$

where $\Delta W_k := \{W_t\}_{t\in[t_k,t_{k+1})}$, and F^u stands for the state transition map derived from (2.1) under a Markov control policy $u : [0,\infty)\times\mathbb{X} \to \mathbb{U}$. From an optimal control perspective, using a Markov policy is not restrictive when the value function has a sufficient smoothness under several technical conditions (see [19, Theorem IV.4.4] and Assumption 1 below). Note that using a piecewise constant control process with a Markov policy u implies that the control

process is given as $U_t = u(\delta(t), X_{\delta(t)})$, for $t \in \mathbb{R}_+$, where $\delta(t) := \lfloor t/\Delta t \rfloor \Delta t$, and the discretized system (2.2) has the Markov property at the discrete times [20].

Safety of the system can be defined by using a safe set $\mathcal{C} \subset \mathbb{X}$. For the discretized system (2.2) and for a given control policy u, the safety probability Ψ^u of the initial state $X_0 = x$ for the outlook horizon $\tau \in \mathbb{R}$ can be characterized as the probability that the state X_k stays within the safe set $\mathcal{C}$ for $k \in \mathcal{N}_\tau := \{0, \ldots, N(\tau)\}$, where $N(\tau) := \lfloor \tau/\Delta t \rfloor$, *i.e.*,

$$\Psi^u(\tau, x) := \mathbb{P}[X_k \in \mathcal{C},\, \forall k \in \mathcal{N}_\tau \mid X_0 = x, u]. \tag{2.3}$$

Then, the objective of this paper can be described as follows.

Problem 1. *Consider the system* (2.2) *starting from an initial state* $x \in \mathcal{C}$. *Then, estimate the maximal safety probability defined as*

$$\Psi^*(\tau, x) := \sup_{u \in \mathcal{U}} \Psi^u(\tau, x), \tag{2.4}$$

where $\mathcal{U}$ *is the class of bounded and Borel measurable Markov control policies.*

For the results stated in the next section, we assume the following technical conditions:

Assumption 1. *We stipulate that*

(a) $\mathbb{U}$ *is compact.*

(b) f, σ *and their first and second partial derivatives with respect to the state are continuous.*

(c) $\sigma(x, u)$ *is an* $n \times n$ *matrix, such that for all* $(x, u) \in \mathbb{X} \times \mathbb{U}$ *and* $\xi \in \mathbb{R}^n$, $\sum_{i,j=1}^n \sigma_{ij}(x, u)\xi_i\xi_j \geq \gamma|\xi|^2$, *where* $\gamma > 0$.

(d) $\mathcal{C}^{\mathrm{c}}$ *is a bounded closed subset of* $\mathbb{X}$ *with* $\partial\mathcal{C}$, *a three-times continuously differentiable manifold.*

(e) $\Psi^u(\tau, x)$ *converges to* $\Psi^u_{\mathrm{c}}(\tau, x) := \mathbb{P}[X_t \in \mathcal{C}, \forall t \in [0, \tau] \,|\, X_0 = x, u]$ *as* $\Delta t \to 0$.

The assumptions (a) to (d) are used for assuring the smoothness of the value function discussed in Sec. 3.2. The assumption (e) is needed to ensure the consistency between the safety probability in the discrete time and the PDE condition in the continuous time, and similar conditions are achieved in [20, 21].

Chapter 3

Proposed Framework

Here we present a physics-informed RL framework for safety probability estimation. For this, a problem formulation with additive cost is presented in Sec. 3.1, and a PDE characterization for the safety probability is derived in Sec. 3.2. The proposed framework is presented in Sec. 3.3.

3.1 Problem Formulation with Additive Cost

Problem 1 can be regarded as a stochastic optimal control problem with a multiplicative cost to be maximized, because the objective function Ψ^u is naively written as follows:

$$\begin{aligned}\Psi^u(\tau, x) =& \mathbb{E}[\mathbb{1}\left[X_k \in \mathcal{C},\, \forall k \in \mathcal{N}_\tau\right] \mid X_0 = x, u] \\ =& \mathbb{E}\left[\prod_{k=0}^{N(\tau)} \mathbb{1}[X_k \in \mathcal{C}] \,\middle|\, X_0 = x, u\right],\end{aligned} \tag{3.1}$$

Remark 1. To convert a multiplicative cost into an additive cost, there are two typical ways taken in RL problem formulations. One is to use a log scale translation of the return. However, this approach fails in the case of the safety probability. This is because each term is conditioned on the previous steps, and thus the reward at the time step k can not be represented as a

function of the state X_k as follows:

$$\begin{aligned}\log \Psi^u(\tau, x) &= \log \mathbb{P}[\cap_{k=0}^{N(\tau)} \mathcal{E}_k | X_0 = x, u] \\ &= \log \mathbb{P}[\mathcal{E}_0 | X_0 = x, u] \, \mathbb{P}[\mathcal{E}_1 | \mathcal{E}_0, X_0 = x, u] \\ &\quad \cdot \mathbb{P}[\mathcal{E}_2 | \mathcal{E}_1, \mathcal{E}_0, X_0 = x, u] \cdots \\ &= \log \prod_{k=0}^{N(\tau)} \mathbb{P}[\mathcal{E}_k | \mathcal{E}_{k-1}, \ldots, \mathcal{E}_0, X_0 = x, u] \\ &= \sum_{k=0}^{N(\tau)} \log \mathbb{P}[\mathcal{E}_k | \mathcal{E}_{k-1}, \ldots, \mathcal{E}_0, X_0 = x, u], \end{aligned} \tag{3.2}$$

where $\mathcal{E}_k$ represents the condition that $X_k \in \mathcal{C}$. The second approach is to augment the state space by considering a sequence of observations as a state, i.e., $\{x_0, x_1, \ldots, x_k\}$. In this paper, we will consider an augmented state that is only one-dimension higher than the original state, which significantly reduces the dimension of the state space.

In this paper, by 1) introducing an appropriate augmented system, and 2) using the idea in [22] of representing the cost in a form of sum of multiplicative costs, we show that the above multiplicative cost can be naturally transformed to an additive cost. For this, we consider a variable H_k that represents the remaining time before the outlook horizon τ is reached, *i.e.*,

$$H_0 = \tau, \quad H_{k+1} = H_k - \Delta t. \tag{3.3}$$

Then, let us consider the augmented state space $\mathcal{S} := \mathbb{R} \times \mathbb{X} \subset \mathbb{R}^{n+1}$ and the augmented state $S_k \in \mathcal{S}$, where we denote the first element of S_k by $\tilde{H}_k$ and the other elements by $\tilde{X}_k$, *i.e.*,

$$S_k = [\tilde{H}_k, \tilde{X}_k^\top]^\top, \tag{3.4}$$

where we use the tilde notation to distinguish between the original dynamics (2.2) and those for the additive cost representation introduced below. For the state S_k, consider the stochastic dynamics starting from the initial state

$$S_0 = s := [\tau, x^\top]^\top \in \mathcal{S} \tag{3.5}$$

with $\tau \in \mathbb{R}$ given as follows: for $\forall k \in \mathbf{Z}_+$,

$$S_{k+1} = \begin{cases} \tilde{F}^u(S_k, \Delta W_k), & S_k \notin \mathcal{S}_{\text{abs}}, \\ S_k, & S_k \in \mathcal{S}_{\text{abs}}, \end{cases} \tag{3.6}$$

with the function $\tilde{F}^u$ given by

$$\tilde{F}^u(S_k, \Delta W_k) := \begin{bmatrix} \tilde{H}_k - \Delta t \\ F^u(\tilde{X}_k, \Delta W_k) \end{bmatrix}, \tag{3.7}$$

and the set of absorbing states $\mathcal{S}_{\mathrm{abs}}$ given by

$$\mathcal{S}_{\mathrm{abs}} := \{[\tilde{\tau}, \tilde{x}^\top]^\top \in \mathcal{S} \mid \tilde{\tau} < 0 \vee \tilde{x} \in \mathcal{C}^{\mathrm{c}}\}. \tag{3.8}$$

The notion of absorbing state is commonly used in RL literature [23], and we have $S_k = [\tilde{H}_k, \tilde{X}_k^\top]^\top = [H_k, X_k^\top]^\top$ for the states satisfying $S_k \notin \mathcal{S}_{\mathrm{abs}}$, but not for $S_k \in \mathcal{S}_{\mathrm{abs}}$ where the state S_k transitions to itself.

Then, the following proposition states that the multiplicative cost representation (3.1) can be transformed to an additive cost by using the augmented dynamics (3.6).

Proposition 1. *Consider the system* (3.6) *starting from an initial state* $s = [\tau, x^\top]^\top \in \mathcal{S}$ *and the reward function* $r : \mathcal{S} \to \mathbb{R}$ *given by*

$$r(S_k) := \mathbf{I}[\tilde{H}_k \in \mathcal{G}]\, \mathbf{I}[S_k \notin \mathcal{S}_{\mathrm{abs}}] \tag{3.9}$$

with $\mathcal{G} := [0, \Delta t)$. *Then, for a given control policy* u, *the value function* v^u *defined by*

$$v^u(s) := \mathbb{E}\left[\sum_{k=0}^{\infty} r(S_k) \;\middle|\; S_0 = s, u\right] \tag{3.10}$$

takes a value in $[0, 1]$ *and is equivalent to the safe probability* $\Psi^u(\tau, x)$, *i.e.,*

$$v^u(s) = \Psi^u(\tau, x). \tag{3.11}$$

Proof. See Appendix A. ■

Since the reward function r contains the term $\mathbf{I}[S_k \notin \mathcal{S}_{\mathrm{abs}}]$, the reward is always zero for $S_k \in \mathcal{S}_{\mathrm{abs}}$. Thus, the value function v^u can also be written as

$$v^u(s) = \mathbb{E}\left[\sum_{k=0}^{N_{\mathrm{f}}} r(S_k) \;\middle|\; S_0 = s, u\right], \tag{3.12}$$

where N_{f} is the first entry time to $\mathcal{S}_{\mathrm{abs}}$ given by

$$N_{\mathrm{f}} := \inf\{j \in \mathbf{Z}_+ \mid S_j \in \mathcal{S}_{\mathrm{abs}}\}. \tag{3.13}$$

Thus, we can consider an episodic RL problem by treating $\mathcal{S}_{\mathrm{abs}}$ as the terminal states. The action-value function $q^u(s,a)$, defined as the value of taking an action $a \in \mathbb{U}$ in state s and thereafter following the policy u, is given by

$$q^u(s,a) := \mathbb{E}\left[\sum_{k=0}^{N_{\mathrm{f}}} r(S_k) \;\middle|\; S_0 = s, U_0 = a, u\right]. \tag{3.14}$$

The objective of RL is to find the optimal action-value function defined as

$$q^*(s,a) := \sup_{u \in \mathcal{U}} q^u(s,a). \tag{3.15}$$

3.2 PDE Characterization of Safety Probability

To implement the technique of PINN, a PDE condition is introduced in this subsection. This is achieved based on the Hamilton-Jacobi-Bellman (HJB) theory of stochastic optimal control for a class of reach-avoid problems [24]. The safety problem can be regarded as a special case of reach-avoid problems, which determines whether there exists a control policy such that the process X reaches a target set A prior to entering an unsafe set B. In [24], for the continuous-time setting of the SDE (2.1), an exit-time problem is considered to characterize the function given by

$$V^{\bar{u}}(t_{\mathrm{s}}, x) := \mathbb{E}[\mathbf{I}[X_{T_{\mathrm{e}}}^{t_{\mathrm{s}},x;\bar{u}} \in A]],\ T_{\mathrm{e}} := \min(T_B, t_{\mathrm{f}}), \tag{3.16}$$

where the process $\{X_t^{t_{\mathrm{s}},x;\bar{u}}\}_{t\in[t_{\mathrm{s}},t_{\mathrm{f}}]}$ represents the unique strong solution of (2.1) for the time interval of $[t_{\mathrm{s}}, t_{\mathrm{f}}]$ starting from the state x under the control process $\bar{u}$, which belongs to the set $\mathcal{U}_{t_{\mathrm{s}}}$ of progressively measurable maps into $\mathbb{U}$. The random variable T_B stands for the first entry time to B. By taking $A := \mathcal{C}$ and $B := \mathcal{C}^{\mathrm{c}}$, the function $V^{\bar{u}}(t_{\mathrm{s}}, x)$ can be rewritten as

$$V^{\bar{u}}(t_{\mathrm{s}}, x) = \mathbb{E}[\mathbf{I}[X_{T_{\mathrm{e}}}^{t_s,x;\bar{u}} \in \mathcal{C}]] \tag{3.17}$$

$$= \mathbb{E}[\mathbf{I}[X_t^{t_s,x;\bar{u}} \in \mathcal{C},\ \forall t \in [t_{\mathrm{s}}, t_{\mathrm{f}}]]], \tag{3.18}$$

where the second equality holds because $\mathbf{I}[X_{T_{\mathrm{e}}}^{t_s,x;\bar{u}} \in \mathcal{C}] = 1$ if and only if the state X_t stays in $\mathcal{C} = B^{\mathrm{c}}$ for $t \in [t_{\mathrm{s}}, t_{\mathrm{f}}]$ (see [24, Proposition 3.3] for a precise discussion). Thus, with Assumption 1(d), we have

$$V^{\bar{u}}(t_{\mathrm{f}} - \tau, x) = \lim_{\Delta t \to 0} \Psi^u(\tau, x) = \lim_{\Delta t \to 0} v^u(s), \tag{3.19}$$

when we choose the control process $\bar{u}$ such that it determines the control input as $U_t = u(t, X_t)$.

In [24], the optimal value function $V^*(t_\mathrm{s}, x) := \sup_{\bar{u}\in\mathcal{U}_{t_\mathrm{s}}} V^{\bar{u}}(t_\mathrm{s}, x)$, is characterized as a solution of an HJB equation. However, it does not admit a classical solution due to the discontinuity of the payoff function given by the indicator function. Instead, V^* becomes a discontinuous viscosity solution of a PDE under mild technical conditions [24, Theorem 4.7]. Furthermore, to allow the use of numerical solution techniques mainly developed for continuous or smooth solutions, it is shown in [24] that one can construct a slightly conservative but arbitrarily precise way of characterizing the original solution by considering a set A_ϵ smaller than A, where $A_\epsilon := \{x \in A \,|\, \mathrm{dist}(x, A^\mathrm{c}) \geq \epsilon\}$, with $\mathrm{dist}(x, A) := \inf_{y\in A} \|x - y\|$. Following [24], to derive a PDE condition to implement PINN, we consider the following function:

$$q_\epsilon^u(s, a) := \mathbb{E}\left[\sum_{k=0}^{N_\mathrm{f}} r_\epsilon(S_k) \;\middle|\; S_0 = s, U_0 = a, u\right], \tag{3.20}$$

where the function r_ϵ is given by

$$r_\epsilon(S_k) := \mathbf{I}[\tilde{H}_k \in \mathcal{G}]\, \mathbf{I}[S_k \notin \mathcal{S}_\mathrm{abs}]\, l_\epsilon(\tilde{X}_k), \tag{3.21}$$

with $\mathcal{C}_\epsilon := \{x \in \mathcal{C} \,|\, \mathrm{dist}(x, \mathcal{C}^\mathrm{c}) \geq \epsilon\}$ and

$$l_\epsilon(x) := \max\left\{1 - \frac{\mathrm{dist}(x, \mathcal{C}_\epsilon)}{\epsilon},\, 0\right\}. \tag{3.22}$$

Theorem 1. *Consider the system* (3.6) *derived from the SDE* (2.1) *and suppose that Assumption 1 holds. Then, for all* $s \in \mathcal{S}$ *and* $a \in \mathbb{U}$, $q^*(s, a) = \lim_{\epsilon\to 0} q_\epsilon^*(s, a)$, *where* $q_\epsilon^*(s, a) := \sup_{u\in\mathcal{U}} q_\epsilon^u(s, a)$. *Furthermore, the function* $q_\epsilon^*(s, a)$ *is the continuous viscosity solution of the following partial differential equation in the limit of* $\Delta t \to 0$*: for* $s \in (0, \infty) \times \mathcal{C}$,

$$\begin{aligned}&\partial_s q_\epsilon^*(s, a^*)\tilde{f}(s, a^*)\\ &\quad + \frac{1}{2}\mathrm{tr}\left[\tilde{\sigma}(s, a^*)\tilde{\sigma}(s, a^*)^\top \partial_s^2 q_\epsilon^*(s, a^*)\right] = 0,\end{aligned} \tag{3.23}$$

where the function $\tilde{f}$ *and* $\tilde{\sigma}$ *are given by*

$$\tilde{f}(s, a) := \begin{bmatrix} -1 \\ f(x, a)\end{bmatrix}, \quad \tilde{\sigma}(s, a) := \begin{bmatrix} 0 \\ \sigma(x, a)\end{bmatrix}, \tag{3.24}$$

and $a^* := \arg\sup_{a\in\mathbb{U}} q^*(s,a)$. *The boundary conditions are given by*

$$q_\epsilon^*([0,x^\top]^\top,a^*) = l_\epsilon(x), \quad \forall x \in \mathbb{X}, \tag{3.25}$$

$$q_\epsilon^*([\tau,x^\top]^\top,a^*) = 0, \quad \forall \tau \in \mathbb{R},\ \forall x \in \partial\mathcal{C}. \tag{3.26}$$

Proof. See Appendix B. ■

Remark 2. Under Assumption 1 and further regularity conditions on the payoff function (i.e., differentiability), the PDE (3.23) can be understood in the classical sense (see e.g., [19, Theorem IV.4.1]). This means that the PDE condition can be imposed by the technique of PINN using automatic differentiation of neural networks.

3.3 Physics-informed RL (PIRL) Framework

Here we present the proposed PIRL framework. While in principle any RL algorithms can be considered, here we focus on an extension of the Deep Q-Network (DQN) algorithm [17] as a simple but practical example. The optimal action-value function $q^*(s,a)$ will be estimated by using a function approximator $Q(s,a;\theta)$ with the parameter θ.

The proposed algorithm is presented in Algorithm 1. The overall structure follows from the DQN algorithm, while we added new statements in the lines 14 to 19 to take samples for PINN and modified the loss function L used in the line 21. Following the framework of PINN [13], our loss function L consists of the three terms of L_D for the data loss of the original DQN, L_P for the physics model given by the PDE (3.23), and L_B for the boundary conditions (3.25) and (3.26), *i.e.*,

$$L = L_\mathrm{D} + \lambda L_\mathrm{P} + \mu L_\mathrm{B}, \tag{3.27}$$

where λ and μ are the weighting coefficients, and the specific form of each loss is given below. After the initializations of the replay memory $\mathcal{D}$, the function approximator Q, and its target function $\hat{Q}$, the main loop starting at the line 4 iterates M episodes, and the inner loop starting at the line 6 iterates the time steps of each episode. Each episode starts with the initialization of the state $s_0 = [h_0, x_0^\top]^\top$ in the line 5, which is sampled from the distribution P_D given by

$$P_\mathrm{D}(s_0) = \begin{cases} 1/|\Omega_\mathrm{D}|, & h_0 = \tau_\mathrm{D} \wedge x_0 \in \Omega_\mathrm{D}, \\ 0, & \text{otherwise}, \end{cases} \tag{3.28}$$

where $\tau_{\mathrm{D}} \in \mathbb{R}_+$ is the time interval of the data acquired through the DQN algorithm, which can be smaller than τ. The set $\Omega_{\mathrm{D}} \subset \mathbb{X}$ is the domain of possible initial states, and $|\Omega_{\mathrm{D}}|$ is its volume. At each time step k, through the lines 7 to 10, a sample of the transition (s_k, a_k, r_k, s'_k) of the state s_k, the action a_k, the reward r_k, and the next state s'_k is stored in the replay memory $\mathcal{D}$. In the lines 11 to 13, a random minibatch $\mathcal{S}_{\mathrm{D}}$ of transitions is taken from $\mathcal{D}$, and the set $\mathcal{Y}_{\mathrm{D}}$ of the target values is calculated using the target q-function $\hat{Q}$, where the j-th element y_j of $\mathcal{Y}_{\mathrm{D}}$ is given by[1]

$$y_j = \begin{cases} r_j, & \text{for terminal } s'_j, \\ r_j + \max_a \hat{Q}(s'_j, a; \hat{\theta}), & \text{otherwise.} \end{cases} \tag{3.29}$$

Then, the loss function L_{D} is given by

$$L_{\mathrm{D}}(\theta; \mathcal{S}_{\mathrm{D}}, \mathcal{Y}_{\mathrm{D}}) = \frac{1}{|\mathcal{S}_{\mathrm{D}}|} \sum_j (y_j - Q(s_j, a_j; \theta))^2. \tag{3.30}$$

To calculate the loss term L_{P}, a random minibatch $\mathcal{S}_{\mathrm{P}} = \{s_l\}$ is taken at the line 15. Each element $s_l = [h_l, x_l^\top]^\top$ is sampled from the distribution P_{P} given by

$$P_{\mathrm{P}}(s_l) = \begin{cases} 1/(\tau|\Omega_{\mathrm{P}}|), & h_l \in [0, \tau] \wedge x_l \in \Omega_{\mathrm{P}}, \\ 0, & \text{otherwise,} \end{cases} \tag{3.31}$$

with $\Omega_{\mathrm{P}} \subset \mathcal{C}$ that specifies the domain where the PDE (3.23) is imposed. In the line 16, the set of greedy actions $\mathcal{A}_{\mathrm{P}} = \{a_l^*\}$ is calculated by $a_l^* = \arg\max_a Q(s_l, a; \theta)$. Then, the PDE loss L_{P} can be defined as

$$L_{\mathrm{P}}(\theta; \mathcal{S}_{\mathrm{P}}, \mathcal{A}_{\mathrm{P}}) = \frac{1}{|\mathcal{S}_{\mathrm{P}}|} \sum_l W_{\mathrm{P}}(s_l, a_l^*; \theta)^2 \tag{3.32}$$

with the residual function $W_{\mathrm{P}}(s_l, a_l^*; \theta)$ given by

$$\begin{aligned} W_{\mathrm{P}}(s_l, a_l^*; \theta) :=& \partial_s Q(s_l, a_l^*; \theta) \tilde{f}(s_l, a_l^*) \\ &+ \frac{1}{2} \mathrm{tr}\left[\tilde{\sigma}(s_l, a_l^*) \tilde{\sigma}(s_l, a_l^*)^\top \partial_s^2 Q(s_l, a_l^*; \theta)\right]. \end{aligned} \tag{3.33}$$

[1]The index j is independent of the time step k. Random sampling from different time steps improves the stability of learning process by reducing non-stationarity and correlation between updates [17].

For the boundary loss L_{B}, as stated in the line 18, a minibatch $\mathcal{S}_{\mathrm{B}} = \{s_m\}$ with $s_m = [h_m, x_m^\top]^\top$ is taken by using the distribution $P_{\mathrm{B}}(s)$ given by

$$P_{\mathrm{B}}(s) = \begin{cases} 1/(2|\Omega_{\mathrm{P}}|), & h_m = 0 \wedge x_m \in \Omega_{\mathrm{P}}, \\ 1/(2\tau|\Omega_{\mathrm{B}}|), & h_m \in [0,\tau] \wedge x \in \Omega_{\mathrm{B}}, \\ 0, & \text{otherwise.} \end{cases} \tag{3.34}$$

where $\Omega_{\mathrm{B}} \subset \partial\mathcal{C}$ stands for the lateral boundary. The loss L_{B} can be defined as

$$L_B(\theta; \mathcal{S}_{\mathrm{B}}, \mathcal{A}_{\mathrm{B}}) = \frac{1}{|\mathcal{S}_{\mathrm{B}}|} \sum_m W_{\mathrm{B}}(s_m, a_m^*; \theta)^2, \tag{3.35}$$

with the set $\mathcal{A}_{\mathrm{B}} = \{a_m^*\}$ of greedy action and the residual W_{B} given by

$$W_{\mathrm{B}}(s_m, a_m^*; \theta) = Q(s_m, a_m^*; \theta) - l_\epsilon(x_m). \tag{3.36}$$

Finally, at the line 21, the parameter θ is updated to minimize the total loss L based on a gradient descent step. The parameter $\hat{\theta}$ of the target function $\hat{Q}$ used in (3.29) is updated at the line 22 with a smoothing factor $\eta \in (0, 1]$.

With this algorithm, the length of each episode scales with the parameter τ_{D}, and it can be chosen as equal to the outlook horizon τ or shorter. When we set $\tau_{\mathrm{D}} < \tau$, the PDE constraint is imposed on the entire time domain of $[0, \tau]$, and the safety probability is learned only from experiences with shorter time interval τ_{D}. In this case, the safety probability predicted by the PINN has bounded error [16, Theorem 6]. This is beneficial in the situation where long-term trajectories for rare unsafe events can be hardly obtained.

Algorithm 1 DQN integrated with PINN

Initialize replay memory $\mathcal{D}$ to capacity N_{mem}
Initialize function Q with random weights θ
Initialize target Q function $\hat{Q}$ with weights $\hat{\theta} = \theta$
for episode $= 1 : M$ **do**
    Initialize state $s_0 = [h_0, x_0^\top]^\top \sim P_{\text{D}}(s_0)$
    for $k = 1 : N_{\text{f}}$ **do**
        /* Emulation of experience */
        With probability ϵ select a random action a_k
        otherwise select $a_k = \arg\max_a Q(s_k, a; \theta)$
        Execute action a_k
        and observe reward r_k and the next state s_{k+1}
        Store transition (s_k, a_k, r_k, s'_k) in $\mathcal{D}$
        /* Sample experiences */
        Sample random minibatch $\mathcal{S}_D$ of
        transitions (s_j, a_j, r_j, s'_j) from $\mathcal{D}$
        Set $\mathcal{Y}_{\text{D}} = \{y_j\}$ as in Eq. (3.29)
        /* Sample minibatch for PDE */
        Sample minibatch $\mathcal{S}_P$ with $s_l \sim P_{\text{P}}(s)$
        Set $\mathcal{A}_{\text{P}}$ with $a_l^* = \arg\max_a Q(s_l, a; \theta)$
        /* Sample minibatch for boundary conditions */
        Sample minibatch $\mathcal{S}_B$ with $s_m \sim P_{\text{B}}(s)$
        Set $\mathcal{A}_{\text{B}}$ with $a_m^* = \arg\max_a Q(s_m, a; \theta)$
        /* Update of weights */
        Perform a gradient descent step on
        loss function L in Eq. (3.27) with respect to θ
        Update target weight $\hat{\theta} \leftarrow \eta\theta + (1 - \eta)\hat{\theta}$
    end for
end for

Chapter 4

Numerical Example

This section demonstrates the effectiveness of the PIRL algorithm through a proof-of-concept numerical example. Consider the SDE (2.1) with the state space $\mathbb{X} := \{x = [x_1, x_2]^\top \,|\, x \in \mathbb{R}^2\}$, the control space $\mathbb{U} := [-1, 1] \subset \mathbb{R}$, and the functions f and σ given by

$$f(x,u) = \begin{bmatrix} -x_1^3 - x_2 \\ x_1 + x_2 + u \end{bmatrix}, \quad \sigma(x,u) = \begin{bmatrix} 0.2 & 0 \\ 0 & 0.2 \end{bmatrix}. \tag{4.1}$$

This example is based on [25] and has an unstable equilibrium point $x^* = [0,0]^\top$, satisfying $f(x^*, 0) = 0$. Here, we consider the safe set $\mathcal{C}$ given as follows[1]:

$$\mathcal{C} = \{x \in \mathbb{X} \,|\, (1 - x_2^2) > 0\}. \tag{4.2}$$

For the implementation of the proposed DQN based algorithm, which admits a discrete action space, the control was restricted to $u \in \{-1.0,\ -0.5,\ 0,\ 0.5,\ 1.0\}$. This restriction does not affect the results when the underlying optimal control problem has a "bang-bang" nature [26]. For the function approximator Q, we used a neural network with 3 hidden layers with 32 units per layer and the hyperbolic tangent (`tanh`) as the activation function. The batch sizes are $|S_{\mathrm{D}}| = |S_{\mathrm{B}}| = |S_{\mathrm{P}}| = 64$, and the weighting coefficients were chosen as $\mu = 1$ and $\lambda = 1 \times 10^{-2}$. The initial state of each episode was randomly sampled from P_{D} with $\Omega_{\mathrm{D}} = \{[x_1, x_2] \in \mathbb{R}^2 \,|\, |x_1| \leq 1.5, |x_2| \leq 1.0\}$. The set Ω_{P} and Ω_{B} were given as $\Omega_{\mathrm{P}} = \{[x_1, x_2] \,|\, |x_1| \leq 1.5, |x_2| \leq 0.9\}$ and

[1] To satisfy Assumption 1(d), one can arbitrarily chose a sufficiently large bounded set $\mathcal{C}^{\mathrm{c}}$ to cover a part of unsafe region in $\mathbb{X}$ of interest.

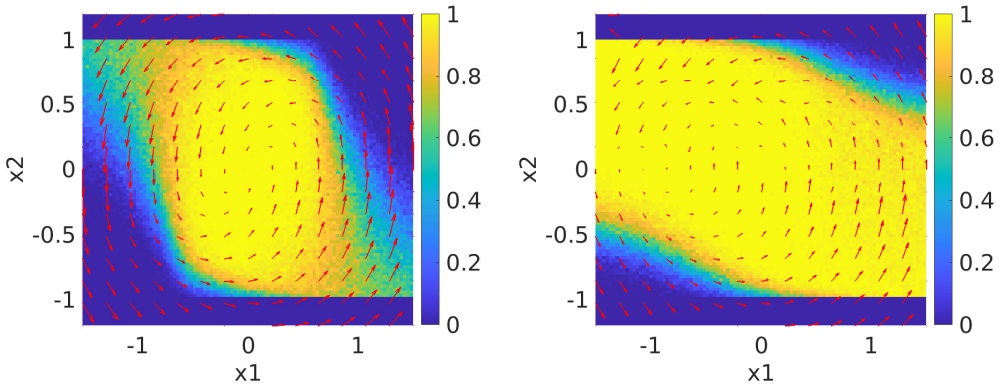

(a) Nominal controller (b) Proposed PIRL

Figure 4.1: Safety probability for the outlook horizon of $\tau = 2.0$.

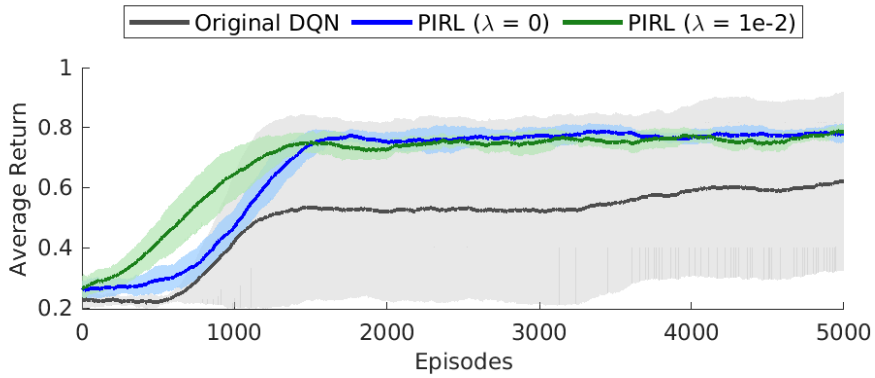

Figure 4.2: Learning progress.

$\Omega_{\mathrm{B}} = \{[x_1, x_2] \,|\, |x_1| \leq 1.5, |x_2| = 1.0\}$, respectively. Our implementation is available at here[2].

Benefit of maximally safe policy and probability. Figure 4.1 shows the safety probability for the outlook horizon $\tau = 2.0$ with (a) nominal controller and (b) controller learned by PIRL. Here, the nominal controller was obtained by using the technique of feedback linearization and then applying the LQR theory as in [25]. The safety probabilities in the figure were calculated by a standard Monte Carlo simulation (the estimation accuracy by the function approximator Q will be discussed later). The red arrows in the figure show the vector field of the deterministic part of the dynamics. When the learned

[2] `https://github.com/hoshino06/PIRL_ACC2024`

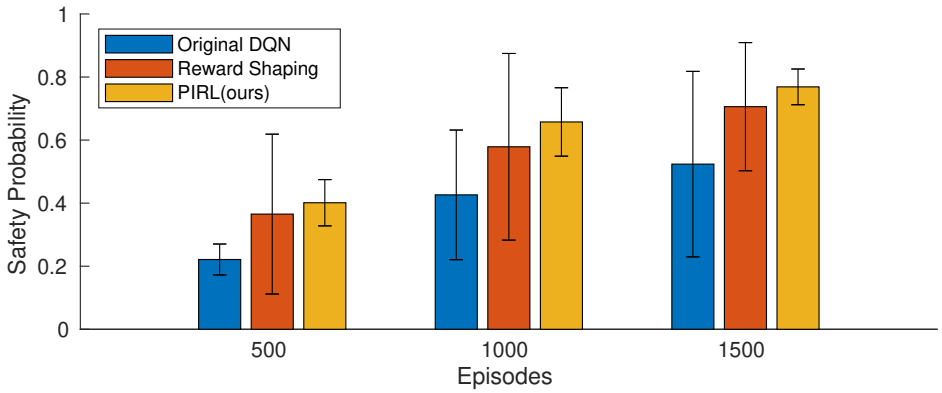

Figure 4.3: Comparison with reward shaping.

policy is used, the system achieves higher safety probability. Thus, when the learned probability is used in probabilistic safety certificates such as [2], it allows the system to explore wider regions.

Efficient learning despite sparse reward. Figure 4.2 shows the training progress. Besides the plot for the proposed PIRL shown by *green*, the *black* line shows the result with the original DQN, and the *blue* line the PIRL with $\lambda = 0$, which means only boundary conditions were imposed. The solid curves correspond to the mean of eight repeated experiments, and the shaded region shows their standard deviation. With the original DQN, the agent has to learn only from sparse zero/one rewards, and often fails to find a safe policy. In contrast, with the proposed PIRL, a safe policy can be found despite the sparse rewards, and the averaged return (corresponds to the safety probability) rises with fewer samples especially at the initial phase.

One of the most common solutions to the issue of sparse reward is reward shaping [27]. For example, one could design a reward r_{rs} to include information about the distance from the boundary of the safe set:

$$r_{\text{rs}}(s) := r(s) + c(1 - x_2^2). \tag{4.3}$$

Figure 4.3 shows the comparison of the averaged safety probability achieved at the initial phase of the training, where $c = 0.05$. It can be seen that the proposed PIRL can learn with fewer experiences as well as the reward shaping. This is because imposing physics loss allows propagation of reward information from neighbors and boundaries, and can serve as an alternative to reward shaping.

Generalization of PIRL. Figure 4.4a shows the accuracy of the safety

probability for $\tau = 2.0$ estimated by the function approximater Q learned with $\tau_{\mathrm{D}} \leq \tau$, with and without PDE condition[3]. The bar plot shows the mean squared error between the output of the learned neural network and the Monte Carlo calculation over 10×10 equally distributed points in the state space, and error bar represents its standard deviation over eight repeated experiments. On the other hand, Fig. 4.4b shows the number of unsafe events during the training process with and without the PDE constraint. By reducing τ_{D}, the number of unsafe events can be reduced, but there is a stringent trade-offs between the estimation accuracy and the length of τ_{D} when the PDE constraint is not imposed ($\lambda = 0$). In contrast, with the proposed PIRL, the safety probability is accurately estimated without acquiring data no longer than τ_{D} while reducing the number of unsafe events. This is beneficial especially in situations when safety must be ensured for a *longer* period than sampled trajectories and when safe actions must be learned *without* sufficiently many rare events and unsafe samples.

[3]Without PDE condition means $\lambda = 0$ but imposing the boundary conditions. With PDE condition, too large λ led to an unstable behavior in the training process due to an excessive exploitation of the greedy policy. Here it was chosen as 5×10^{-3} for $\tau_{\mathrm{D}} = 1.5$ and 3×10^{-3} for $\tau_{\mathrm{D}} = 1.0$ to avoid an unstable behavior in the training process.

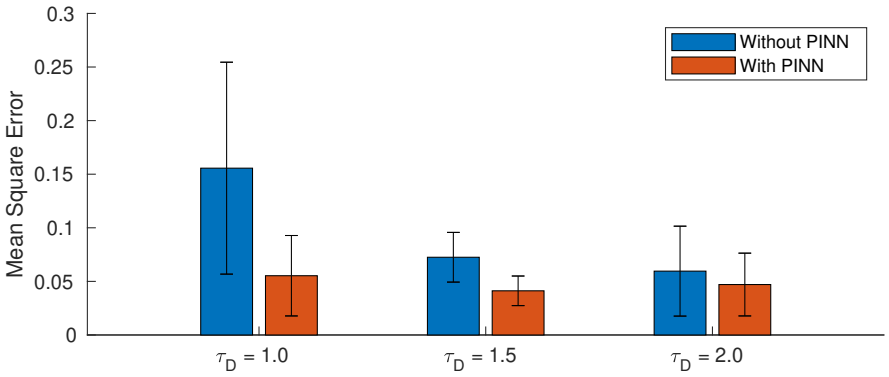

(a) Estimation accuracy for $\tau = 2.0$

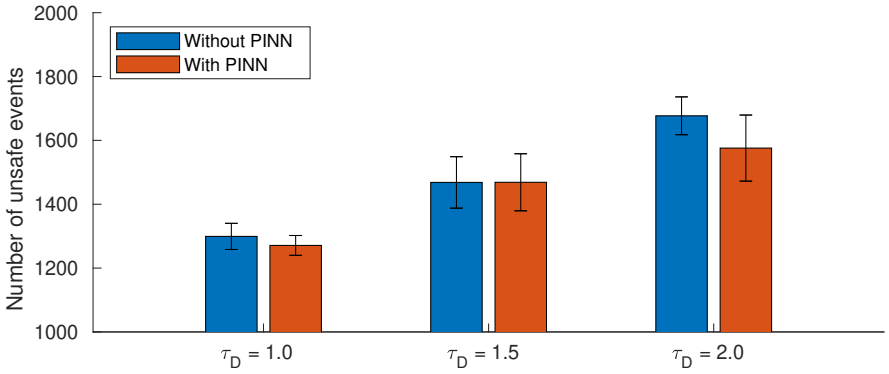

(b) Number of unsafe events

Figure 4.4: Results of generalization with $\tau_{\mathrm{D}} \leq \tau$.

Chapter 5

Conclusions

In this paper, we proposed a Physics-informed Reinforcement Learning (PIRL) for efficiently estimating the safety probability under maximally safe actions. This was based on the exact characterization of the safety probability as the value function of an RL problem and the derivation of a PDE condition satisfied by the action-value function. The effectiveness of PIRL has been demonstrated through an example based on the Deep Q-Network algorithm integrated with the technique of Physics-informed Neural Network (PINN). Future work includes application of this framework to estimate safety probability in real-world tasks such as autonomous driving, and its use in *e.g.*, safe RL.

Chapter 6

Proofs

6.1 Proof of Proposition 1

Proof. From the fact that $\tilde{H}_k = H_k$ and $\tilde{X}_k = X_k$ hold for $S_k \notin \mathcal{S}_{\text{abs}}$, the safety probability $\Psi^u(\tau, x)$ can be rewritten as follows:

$$\Psi^u(\tau, x) = \mathbb{E}\left[P_{N(\tau)} \,\middle|\, S_0 = s, u\right] \tag{6.1}$$

with the symbol P_k is defined as

$$P_k := \prod_{j=0}^{k} \mathbb{1}[\tilde{X}_j \in \mathcal{C}]. \tag{6.2}$$

Then, this can be further transformed into a form of sum of multiplicative cost as follows:

$$\begin{aligned}\Psi^u(\tau, x) =& \mathbb{E}\left[\left(P_{N(\tau)}\right) \mathbb{1}[\tilde{H}_N \in \mathcal{G}] \,\middle|\, S_0 = s, u\right] \\ =& \mathbb{E}\left[\sum_{k=0}^{N(\tau)} \left(P_k\right) \mathbb{1}[\tilde{H}_k \in \mathcal{G}] \,\middle|\, S_0 = s, u\right].\end{aligned} \tag{6.3}$$

Here, the transformations from (6.1) to (6.3) is based on the fact that $\mathbf{I}[\tilde{H}_k \in \mathcal{G}]$ is 1 if $k = N(\tau)$ and 0 otherwise. Given this form of representation, the proof will be completed by showing that the expectation of the return $G = \sum_{k=0}^{\infty} r(S_k)$ is equal to (6.3). First, consider the case where $\tilde{X}_k$ stays

inside the safe set $\mathcal{C}$ for all $k = 0, \ldots, N(\tau)$, *i.e.*, the trajectory is safe. In this case, we have

$$P_k = 1, \quad \mathbf{I}[S_k \notin \mathcal{S}_{\text{abs}}] = 1, \quad \forall k \in \{0, \ldots, N(\tau)\}. \tag{6.4}$$

Since $\mathbf{I}[\tilde{H}_k \in \mathcal{G}] = 0$ for all $k \geq N(\tau) + 1$, we have

$$\begin{aligned} G &= \sum_{k=0}^{\infty} \mathbf{I}[\tilde{H}_k \in \mathcal{G}]\, \mathbf{I}[S_k \notin \mathcal{S}_{\text{abs}}] \\ &= \sum_{k=0}^{N(\tau)} \mathbb{1}[\tilde{H}_k \in \mathcal{G}]\, \mathbf{I}[S_k \notin \mathcal{S}_{\text{abs}}] \\ &= \sum_{k=0}^{N(\tau)} (P_k)\, \mathbb{1}[\tilde{H}_k \in \mathcal{G}]. \end{aligned} \tag{6.5}$$

Next, consider the case where $\tilde{X}_{\bar{k}} \notin \mathcal{C}$ for some $\bar{k} \in \{0, \ldots, N(\tau)\}$, *i.e.*, the trajectory is unsafe. Then, we have

$$P_k = \mathbf{I}[S_k \notin \mathcal{S}_{\text{abs}}] = 1, \quad \forall k \in \{0, \ldots, \bar{k} - 1\}, \tag{6.6}$$

$$P_k = \mathbf{I}[S_k \notin \mathcal{S}_{\text{abs}}] = 0, \quad \forall k \in \{\bar{k}, \ldots, N(\tau)\}. \tag{6.7}$$

Thus, the return becomes

$$\begin{aligned} G &= \sum_{k=0}^{N(\tau)} \mathbb{1}[\tilde{H}_k \in \mathcal{G}]\, \mathbf{I}[S_k \notin \mathcal{S}_{\text{abs}}] \\ &= \sum_{k=0}^{\bar{k}-1} \mathbb{1}[\tilde{\tau}_k \in \mathcal{G}] + \sum_{k=\bar{k}}^{N(\tau)} 0 \cdot \mathbb{1}[\tilde{H}_k \in \mathcal{G}] \\ &= \sum_{k=0}^{N(\tau)} (P_k)\, \mathbb{1}[\tilde{H}_k \in \mathcal{G}]. \end{aligned} \tag{6.8}$$

Thus, the expectation of the return G over all possible trajectories, which is represented either by (6.5) or (6.8), is equivalent to the safety probability Ψ^u given in (6.3). Also, the function v^u takes a value in $[0, 1]$, since the return G takes 0 or 1. ■

6.2 Proof of Theorem 1

Proof. First, consider the following function for the SDE (2.1) with the exit-time $T_{\mathrm{e}} = \min(T_{\mathcal{C}^{\mathrm{c}}}, t_{\mathrm{f}})$:

$$V_\epsilon^{\bar{u}}(t_{\mathrm{s}}, x) := \mathbb{E}[l_\epsilon(X_{T_{\mathrm{e}}}^{t_{\mathrm{s}},x;\bar{u}})]. \tag{6.9}$$

Then, it follows from [24, Theorem 4.7] that under Assumption 1(a)-(d), the function $V_\epsilon^*(t_{\mathrm{s}}, x) := \sup_{\bar{u}\in\mathcal{U}_{t_{\mathrm{s}}}} V_\epsilon^{\bar{u}}(t_{\mathrm{s}}, x)$ is a viscosity solution of the following PDE:

$$\sup_{a\in\mathbb{U}} \mathcal{L}^a V_\epsilon^*(t_{\mathrm{s}}, x) = 0, \quad \forall (t_{\mathrm{s}}, x) \in [0, t_{\mathrm{f}}) \times \mathcal{C}, \tag{6.10}$$

where $\mathcal{L}^a$ is the Dynkin operator defined as

$$\begin{aligned}\mathcal{L}^a \Phi(t, x) :=& \partial_t \Phi(t, x) + f(x, a)^\top \partial_x \Phi(t, x) \\ &+ \frac{1}{2}\mathrm{tr}[\sigma(x, a)\sigma(x, a)^\top \partial_x^2 \Phi(t, x)],\end{aligned} \tag{6.11}$$

and the boundary condition given by

$$V_\epsilon^*(t_{\mathrm{s}}, x) = l_\epsilon(x), \quad \forall (t, x) \in [0, t_{\mathrm{f}}] \times \mathcal{C}^{\mathrm{c}} \cup \{t_{\mathrm{f}}\} \times \mathbb{R}^n. \tag{6.12}$$

The continuity of the function V_ϵ^* follows from Lipschitz continutity of the payoff function l_ϵ and uniform continuity of the stopped solution process [24, Proposition 4.8].

Here, the function $V_\epsilon^{\bar{u}}(t_{\mathrm{s}}, x)$ can be rewritten as

$$\begin{aligned}V_\epsilon^{\bar{u}}(t_{\mathrm{s}}, x) &= \mathbb{E}[\mathbf{I}[X_{T_{\mathrm{e}}}^{t_s,x;\bar{u}} \in \mathcal{C}]\, l_\epsilon(X_{T_{\mathrm{e}}}^{t,x;\bar{u}})] \\ &= \mathbb{E}[\mathbf{I}[X_t^{t_s,x;\bar{u}} \in \mathcal{C},\, \forall t \in [t_{\mathrm{s}}, t_{\mathrm{f}}]]\, l_\epsilon(X_{T_{\mathrm{e}}}^{t,x;\bar{u}})],\end{aligned}$$

where the above transformations follows from the fact that $l_\epsilon(X_{T_{\mathrm{e}}}^{t_{\mathrm{s}},x;\bar{u}}) \neq 0$ only if $X_{T_{\mathrm{e}}}^{t_{\mathrm{s}},x;\bar{u}} \in \mathcal{C}$. Then, with the function $\Psi_\epsilon^u(\tau, x)$ given by

$$\Psi_\epsilon^u(\tau, x) := \mathbb{E}\left[\prod_{k=0}^{N(\tau)} \mathbf{I}[X_k \in \mathcal{C}]\, l_\epsilon(X_{N(\tau)}) \,\middle|\, X_0 = x, u\right],$$

from the continuity of the function l_ϵ and Assumption 1(e), we have $V_\epsilon^u(t_\mathrm{f} - \tau, x) = \lim_{\Delta t \to 0} \Psi_\epsilon^u(\tau, x)$. Furthermore, with the same arguments as in the proof of Proposition 1, we have $\Psi_\epsilon^u(\tau, x) = v_\epsilon^u(s)$ with

$$v_\epsilon^u(s) := \mathbb{E}\left[\sum_{k=0}^{N(\tau)} r_\epsilon(S_k) \;\middle|\; S_0 = s, u \right]. \tag{6.13}$$

Since we have

$$v_\epsilon^u(s) = \max_{a \in \mathbb{U}} q_\epsilon^*(s, a) \xrightarrow[\Delta t \to 0]{} V_\epsilon^*(t_\mathrm{f} - \tau, x), \tag{6.14}$$

and $V_\epsilon^*(t_\mathrm{s}, x)$ satisfies the PDE (6.10), the function $q_\epsilon^*(s, a)$ satisfies the following PDE as $\Delta t \to 0$:

$$\begin{aligned} &\sup_{a \in \mathcal{U}} \partial_s q_\epsilon^*(s, a^*) \tilde{f}(s, a) \\ &\qquad + \frac{1}{2} \mathrm{tr}\left[\tilde{\sigma}(s, a) \tilde{\sigma}(s, a)^\top \partial_s^2 q_\epsilon^*(s, a^*) \right] = 0. \end{aligned} \tag{6.15}$$

Here, from $q_\epsilon^*(s, a) = r_\epsilon(s) + \mathbb{E}[v_\epsilon^*(s')|s, a]$, where s' is the next state given the current state s and the input a, we have

$$\begin{aligned} a^* &= \arg\sup_{a \in \mathbb{U}} \; r(s) + \mathbb{E}[v_\epsilon^*(s')|s, a] \\ &= \arg\sup_{a \in \mathbb{U}} \mathbb{E}[v_\epsilon^*(s')|s, a] \\ &= \arg\sup_{a \in \mathbb{U}} \frac{\mathbb{E}[v_\epsilon^*(s')|s, a] - v_\epsilon^*(s)}{\Delta t} \end{aligned} \tag{6.16}$$

where the above transformation is based on the fact that $r_\epsilon(s)$ and v_ϵ^* are independent of a. Thus, from the Ito's Lemma, a^* maximizes the right-hand side of (6.15) as $\Delta t \to 0$, and substituting a^* gives (3.23):

$$\begin{aligned} &\partial_s q_\epsilon^*(s, a^*) \tilde{f}(s, a^*) \\ &\quad + \frac{1}{2} \mathrm{tr}\left[\tilde{\sigma}(s, a^*) \tilde{\sigma}(s, a^*)^\top \partial_s^2 q_\epsilon^*(s, a^*) \right] = 0. \end{aligned}$$

■

Bibliography

[1] M. P. Chapman, J. Lacotte, A. Tamar, D. Lee, K. M. Smith, V. Cheng, J. F. Fisac, S. Jha, M. Pavone, and C. J. Tomlin, "A risk-sensitive finite-time reachability approach for safety of stochastic dynamic systems," in *2019 American Control Conference (ACC)*, 2019, pp. 2958–2963.

[2] Z. Wang, H. Jing, C. Kurniawan, A. Chern, and Y. Nakahira, "Myopically verifiable probabilistic certificate for long-term safety," in *2022 American Control Conference (ACC)*, Jun. 2022, pp. 4894–4900.

[3] F. M. F. Berkenkamp, "Safe exploration in reinforcement learning: Theory and applications in robotics," Ph.D. dissertation, ETH Zurich, 2019.

[4] Y. Kim, R. Allmendinger, and M. López-Ibáñez, "Safe learning and optimization techniques: Towards a survey of the state of the art," in *Trustworthy AI - Integrating Learning, Optimization and Reasoning*. Springer International Publishing, 2021, pp. 123–139.

[5] K. Srinivasan, B. Eysenbach, S. Ha, J. Tan, and C. Finn, "Learning to be safe: Deep RL with a safety critic," *arXiv: 2010.14603 [cs.LG]*, Oct. 2020.

[6] Z. Qin, Y. Chen, and C. Fan, "Density constrained reinforcement learning," in *Proceedings of the 38th International Conference on Machine Learning*, 2021, pp. 8682–8692.

[7] W. Chen, D. Subramanian, and S. Paternain, "Policy gradients for probabilistic constrained reinforcement learning," in *57th Annual Conference on Information Sciences and Systems*, 2023, pp. 1–6.

[8] B. Thananjeyan, A. Balakrishna, S. Nair, M. Luo, K. Srinivasan, M. Hwang, J. E. Gonzalez, J. Ibarz, C. Finn, and K. Goldberg, "Recov-

ery rl: Safe reinforcement learning with learned recovery zones," *IEEE Robotics and Automation Letters*, vol. 6, no. 3, pp. 4915–4922, 2021.

[9] J. Zhang, "Modern monte carlo methods for efficient uncertainty quantification and propagation: A survey," *WIREs Computational Statistics*, vol. 13, no. 5, p. e1539, 2021.

[10] J. F. Fisac, N. F. Lugovoy, V. Rubies-Royo, S. Ghosh, and C. J. Tomlin, "Bridging Hamilton-Jacobi safety analysis and reinforcement learning," in *2019 International Conference on Robotics and Automation (ICRA)*, May 2019, pp. 8550–8556.

[11] A. Tamar, Y. Chow, M. Ghavamzadeh, and S. Mannor, "Policy gradient for coherent risk measures," *Adv. Neural Inf. Process. Syst.*, vol. 28, 2015.

[12] A. Abate, M. Prandini, J. Lygeros, and S. Sastry, "Probabilistic reachability and safety for controlled discrete time stochastic hybrid systems," *Automatica*, vol. 44, no. 11, pp. 2724–2734, Nov. 2008.

[13] M. Raissi, P. Perdikaris, and G. E. Karniadakis, "Physics-informed neural networks: A deep learning framework for solving forward and inverse problems involving nonlinear partial differential equations," *J. Comput. Phys.*, vol. 378, pp. 686–707, Feb. 2019.

[14] S. Cai, Z. Mao, Z. Wang, M. Yin, and G. E. Karniadakis, "Physics-informed neural networks (PINNs) for fluid mechanics: a review," *Acta Mech. Sin.*, vol. 37, no. 12, pp. 1727–1738, Dec. 2021.

[15] S. Cuomo, V. S. Di Cola, F. Giampaolo, G. Rozza, M. Raissi, and F. Piccialli, "Scientific machine learning through Physics–Informed neural networks: Where we are and what's next," *J. Sci. Comput.*, vol. 92, no. 3, p. 88, Jul. 2022.

[16] Z. Wang and Y. Nakahira, "A generalizable physics-informed learning framework for risk probability estimation," in *Proceedings of the 5th Annual Learning for Dynamics and Control Conference (L4DC)*, 2023, pp. 358–370.

[17] V. Mnih, K. Kavukcuoglu, D. Silver, A. Graves, I. Antonoglou, D. Wierstra, and M. Riedmiller, "Playing atari with deep reinforcement learning," *arXiv: 1312.5602 [cs.LG]*, Dec. 2013.

[18] C. Banerjee, K. Nguyen, C. Fookes, and M. Raissi, "A survey on physics informed reinforcement learning: Review and open problems," *arXiv: 2309.01909 [cs.LG]*, Sep. 2023.

[19] W. H. Fleming and H. M. Soner, *Controlled Markov Processes and Viscosity Solutions*, 2nd ed. Springer, 2006.

[20] X. Mao, "Stabilization of continuous-time hybrid stochastic differential equations by discrete-time feedback control," *Automatica*, vol. 49, no. 12, pp. 3677–3681, 2013.

[21] E. Bayraktar and A. D. Kara, "Approximate q learning for controlled diffusion processes and its near optimality," *SIAM Journal on Mathematics of Data Science*, vol. 5, no. 3, pp. 615–638, 2023.

[22] S. Summers and J. Lygeros, "Verification of discrete time stochastic hybrid systems: A stochastic reach-avoid decision problem," *Automatica*, vol. 46, no. 12, pp. 1951–1961, Dec. 2010.

[23] R. S. Sutton and A. G. Barto, *Reinforcement Learning: An Introduction*, 2nd ed. Cambridge, MA: MIT Press, 2018.

[24] P. Mohajerin Esfahani, D. Chatterjee, and J. Lygeros, "The stochastic reach-avoid problem and set characterization for diffusions," *Automatica*, vol. 70, pp. 43–56, 2016.

[25] R. W. Beard, G. N. Saridis, and J. T. Wen, "Galerkin approximations of the generalized hamilton-jacobi-bellman equation," *Automatica*, vol. 33, no. 12, pp. 2159–2177, 1997.

[26] V. Rubies-Royo, D. Fridovich-Keil, S. Herbert, and C. J. Tomlin, "A classification-based approach for approximate reachability," in *2019 International Conference on Robotics and Automation (ICRA)*, May 2019, pp. 7697–7704.

[27] Nilaksh, A. Ranjan, S. Agrawal, A. Jain, P. Jagtap, and S. Kolathaya, "Barrier functions inspired reward shaping for reinforcement learning," *arXiv: 2403.01410 [cs.RO]*, 2024.

Appendix A

Research Products for This Project

- Hikaru Hoshino and Yorie Nakahira, "Physics-informed RL for Maximal Safety Probability Estimation." American Control Conference (ACC), Toronto, ON, Canada, 2024, pp. 3576-3583.
- Hikaru Hoshino, Jiaxing Li, Arnav Menon, John M. Dolan, and Yorie Nakahira, "Autonomous Drifting Based on Maximal Safety Probability Learning." The 27th IEEE International Conference on Intelligent Transportation Systems.
- Zhuoyuan Wang, Reece Keller, Xiyu Deng, Kenta Hoshino, Takashi Tanaka, and Yorie Nakahira, "Physics-informed representation and learning: Control and risk quantification." In Proceedings of the AAAI Conference on Artificial Intelligence, vol. 38, no. 19, pp. 21699-21707. 2024.
- Zhuoyuan Wang, Albert Chern, and Yorie Nakahira. "Generalizable Physics-informed Learning for Stochastic Safety-critical Systems." arXiv preprint arXiv:2407.08868, 2024.

1. Report No. 471	2. Government Accession No.	3. Recipient's Catalog No.
4. Title and Subtitle *Safe Decision-Making in Uncertainty Environment*		**5. Report Date** July 31st, 2024
		6. Performing Organization code
7. Author(s) Yorie Nakahira (PI) (https://orcid.org/0000-0003-3324-4602) Hiraku Hoshino (https://orcid.org/0000-0003-2487-8320)		**8. Performing Organization Report No.**
9. Performing Organization Name and Address Carnegie Mellon University 5000 Forbes Avenue Pittsburgh, PA 15213		**10. Work Unit No.**
		11. Contract or Grant No. Federal Grant No. 69A3552344811
12. Sponsoring Agency Name and Address Safety21 University Transportation Center Carnegie Mellon University 5000 Forbes Avenue Pittsburgh, PA 15213		**13. Type of Report and Period Covered** Final Report (July 1, 2023-June 30, 2024)
		14. Sponsoring Agency Code USDOT

15. Supplementary Notes
Related and subsequent publications.

Hikaru Hoshino, Jiaxing Li, Arnav Menon, John M. Dolan, and Yorie Nakahira. Autonomous Drifting Based on Maximal Safety Probability Learning. The 27th IEEE International Conference on Intelligent Transportation Systems.

Zhuoyuan Wang, Reece Keller, Xiyu Deng, Kenta Hoshino, Takashi Tanaka, and Yorie Nakahira. Physics-informed representation and learning: Control and risk quantification. In Proceedings of the AAAI Conference on Artificial Intelligence, vol. 38, no. 19, pp. 21699-21707. 2024.

Zhuoyuan Wang, Albert Chern, and Yorie Nakahira. Generalizable Physics-informed Learning for Stochastic Safety-critical Systems. arXiv preprint arXiv:2407.08868, 2024.

16. Abstract
This report introduces techniques for safe autonomous driving in uncertain and interactive environments. The proposed methods have the following merits.
1. Risk Quantification and Reachability: Accurate risk estimation is essential for safe control and learning, particularly in environments where uncertain or interactive elements are involved. The proposed method quantifies long-term safety probabilities, even in scenarios with limited samples from risky states or long-term trajectories. This is crucial for avoiding potentially hazardous situations without requiring extensive data.
2. Maximally Safe Actions: By focusing on the maximal safety probability, the method helps in selecting actions that are safe without being overly conservative. This reduces the likelihood of overly cautious behavior, which could impair the performance of autonomous driving systems in real-world, dynamic environments.
3. Physics-Informed Reinforcement Learning (PIRL): The PIRL algorithm introduces physics constraints into the learning process, which enhances safety in complex and interactive environments. These constraints propagate risk information to neighboring states, allowing the system to infer risk in unsampled or rare states, enhancing the robustness of the driving system in uncertain situations.
These methods will be useful for autonomous vehicles to make informed and safe decisions that minimizing risks while maximizing performance, even in environments with uncertain agents.

17. Key Words Safety, control, risk quantification, uncertainty		18. Distribution Statement No restrictions.	
19. Security Classif. (of this report) Unclassified	**20. Security Classif. (of this page)** Unclassified	**21. No. of Pages** 30	**22. Price** -

Form DOT F 1700.7 (8-72) Reproduction of completed page authorized